



NEWS & VIEWS

Is Low Alveolar Type II Cell *SOD3* in the Lungs of Elderly Linked to the Observed Severity of COVID-19?

Ahmed S. Abouhashem,^{1,*} Kanhaiya Singh,^{1,*} Hassan M.E. Azzazy,² and Chandan K. Sen¹

Abstract

Human lungs single-cell RNA sequencing data from healthy donors (elderly and young; GEO accession no. GSE122960) were analyzed to isolate and specifically study gene expression in alveolar type II cells. Colocalization of angiotensin-converting enzyme 2 (*ACE2*) and *TMPRSS2* enables severe acute respiratory syndrome coronavirus 2 (SARS-CoV 2) to enter the cells. Expression levels of these genes in the alveolar type II cells of elderly and young patients were comparable and, therefore, do not seem to be responsible for worse outcomes observed in coronavirus disease 2019 (COVID-19) affected elderly. In cells from the elderly, 263 genes were downregulated and 95 upregulated. Superoxide dismutase 3 (*SOD3*) was identified as the top-ranked gene that was most downregulated in the elderly. Other redox-active genes that were also downregulated in cells from the elderly included activating transcription factor 4 (*ATF4*) and metallothionein 2A (*M2TA*). *ATF4* is an endoplasmic reticulum stress sensor that defends lungs *via* induction of heme oxygenase 1. The study of downstream factors known to be induced by *ATF4*, according to Ingenuity Pathway Analysis™, identified 24 candidates. Twenty-one of these were significantly downregulated in the cells from the elderly. These downregulated candidates were subjected to enrichment using the Reactome Database identifying that in the elderly, the ability to respond to heme deficiency and the *ATF4*-dependent ability to respond to endoplasmic reticulum stress is significantly compromised. *SOD3*-based therapeutic strategies have provided beneficial results in treating lung disorders including fibrosis. The findings of this study propose the hypotheses that lung-specific delivery of *SOD3/ATF4*-related antioxidants will work in synergy with promising antiviral drugs such as remdesivir to further improve COVID-19 outcomes in the elderly. *Antioxid. Redox Signal.* 33, 59–65.

Keywords: COVID19, single-cell RNA sequencing, lung, ROS, *SOD3*, *ATF4*

Introduction

THE HUMAN LUNG ALVEOLAR EPITHELIUM is mainly composed of types I/II alveolar cells and macrophages. In contrast with alveolar type I cells, alveolar type II cells are capable of giving rise to both type II and type I alveolar cells (18). Alveolar type II cells serve many critical functions including production of pulmonary surfactant, stabilization of airway epithelial barrier, local immune defense, and airway regeneration after injury. As one of few cells in the human body that coexpresses angiotensin-converting enzyme 2

Innovation

For the first time, single-cell RNA sequencing data of the human lungs have been studied as a function of age to reveal that age-related weakening of specific components of the antioxidant defense system of the alveolar type II cells should be tested for a mechanistic connection of COVID-19 severity outcomes.

¹Indiana Center for Regenerative Medicine and Engineering, Department of Surgery, Indiana University School of Medicine, Indianapolis, Indiana, USA.

²Department of Chemistry, School of Sciences and Engineering, The American University in Cairo, New Cairo, Egypt.

*These authors contributed equally to this study.

(ACE2) receptor and the TMPRSS2 protease, required for attachment and cellular entry of coronavirus disease 2019 (COVID-19), alveolar type II cells are readily targeted by coronavirus 2 (severe acute respiratory syndrome coronavirus 2 [SARS-CoV 2]) (8). COVID-19 is an emerging respiratory disease caused by SARS-CoV 2. Most COVID-19⁺ patients exhibit mild to moderate symptoms, with ~10% developing acute respiratory distress syndrome, which is the leading cause of mortality among these patients (9). Histopathologic changes of the lungs related to COVID-19 include diffuse alveolar damage, chronic inflammatory infiltrates, and intra-alveolar fibrinous exudates (30). The severity of symptoms and mortality of elderly patients are higher than those of younger patients (14).

Reactive oxygen species (ROS) and reactive nitrogen species (RNS) are known to be produced by cells of the innate immune system and others in response to viral infection (11). ROS/RNS are directly implicated in lung fibrosis and declining lung function (5). Antioxidant enzymes such lecithinized superoxide dismutase (SOD) have proven to be useful in patients suffering from lung fibrosis (25). There is substantial literature demonstrating a causative role of ROS/RNS in the development of lung fibrosis (21). In virus-induced lung disease, antioxidant treatment attenuated lung inflammation and airway hyper-reactivity (3). In this study, we utilized single-cell sequencing data from elderly and younger humans to specifically study alveolar type II cells to identify genes that are most profoundly affected as a function of age. Such effort was intended at developing novel hypotheses to understand why lungs of the elderly are more severely affected in COVID-19.

Results

Human lungs single-cell RNA sequencing (scRNA-seq) data from four healthy donors (9783 cells from old-age group, 57 and 63 years old, and 8501 cells from young-age group, 22 and 29 years old; GEO accession no. GSE122960) were analyzed (20). Analysis of scRNA-seq data generated 14 clusters visualized using t-distributed stochastic neighbor embedding (t-SNE). Such clustering was based on a nonlinear dimensionality reduction technique for embedding high-dimensional data with the objective of visualization in low-dimensional space. As depicted in Figure 1A, these clusters include epithelial cells (alveolar type II cells), macrophages in different states, epithelial cells (alveolar type I cells), monocytes, B cells, T cells/NK cells, endothelial cells, and stem cells. SingleR package in R (1), in conjunction with the Human Primary Cell Atlas (HPCA) data set, was used to identify alveolar type II cells from the total lung cell population. These cells heavily expressed the characteristic surfactant protein C gene (Supplementary Fig. 1A, B). Genes of this particular alveolar type II cell cluster were analyzed for differential expression as a function of aging (Fig. 1B). Colocalization of *ACE2* and *TMPRSS2* enables SARS-CoV 2 to enter the cells (8). Expression levels of these genes in the alveolar type II cells of old and young patients were comparable (Fig. 1C) and, therefore, do not seem to be responsible for worse outcomes in COVID-19-affected elderly.

Compared with that in alveolar type II cells from younger donors, in cells of older donors, 263 genes were differentially downregulated and 95 genes were upregulated (adjusted *p*-value <0.05 and 10% log fold change; Fig. 1D, Supple-

mentary Table S1). *SOD3* was identified as the top-ranked (by log of fold change) gene that was most downregulated in alveolar type II cells (Supplementary Table S1). This observation piqued our interest in other genes with known redox functions. Other genes with known redox-based functions that were also downregulated in alveolar type II cells of elderly lung donors included activating transcription factor 4 (*ATF4*) and metallothionein 2A (*M2TA*) (Fig. 2A–C). Additional studies to look for *SOD3*-interacting genes, as predicted by String database (String version 11.0), recognized the following: *SOD2*, catalase (*CAT*), glutathione peroxidase 1 (*GPX1*), *GPX2*, *GPX3*, *GPX5*, *GPX7*, *GPX8*, antioxidant 1 copper chaperone (*ATOX1*), and ATPase copper transporting alpha (*ATP7A*) (Supplementary Fig. 2A, B). Among these candidates, *GPX1* was the only gene that was differentially low in expression in cells from elderly donors (Supplementary Fig. S2B, Supplementary Table S1). Viral infection is known to employ endoplasmic reticulum (ER) stress to cause lung fibrosis (12). *ATF4*, an ER stress sensor that can defend lungs *via* induction of heme oxygenase 1, was downregulated in alveolar type II cells of the elderly (Fig. 2B). Study of downstream factors that are known to be induced by *ATF4*, according to Ingenuity Pathway Analysis™ (IPA), identified 24 candidates. Twenty-one of these 24 were significantly downregulated in the alveolar type II cells of the elderly (Fig. 2C). The downregulated candidates were subjected to pathway enrichment using the Reactome Database. These analyses identified that in the elderly, the ability to respond to heme deficiency and the *ATF4*-dependent ability to respond to endoplasmic reticulum stress are significantly compromised (Fig. 2D, Table 1).

Discussion

At the time of this reporting, of 13,130 COVID-19 deaths (of reported death from all causes 582,565 on April 19, 2020) in the United States as reported by the Center for Disease Control, 13,001 decedents were of age 35 years or above, representing 99% of all COVID-19 deaths. Decedents aged 55 years or above account for 91% of all COVID-19 deaths (19). The younger donors of this study were both <30 years, whereas the elderly donors were both >55 years (19). In brief, the SARS-CoV 2 virion contains four proteins: spike, envelope, membrane, and nucleocapsid, and a single-stranded RNA. The virion binds to ACE2 receptor located on alveolar type II cells making these cells a target for infection. Once SARS-CoV 2 has attached to these receptors, the TMPRSS2 protease cleaves the spike protein to expose a fusion peptide that helps the virus enter the cell (8). This enables the virions to release their RNA into infected cells. Coexpression of ACE2 and TMPRSS2 on type II cells makes them a preferred site for SARS-CoV 2 attachment, entry, and replication (16). In late stages of the severe form of COVID-19, cytokine storm has been evident (17). Under these conditions, when the inflammatory system has gone awry in COVID-19–unrelated pathologies, there is ample evidence of oxidative stress (15). Findings of this study, involving an unbiased query of differentially expressed genes specifically in alveolar type II cells of the human lung, point toward specific elements of the antioxidant defense system that are weakened as a function of age. *SOD3*-deficient mice develop severe lung damage in the presence of normal oxygen tension along

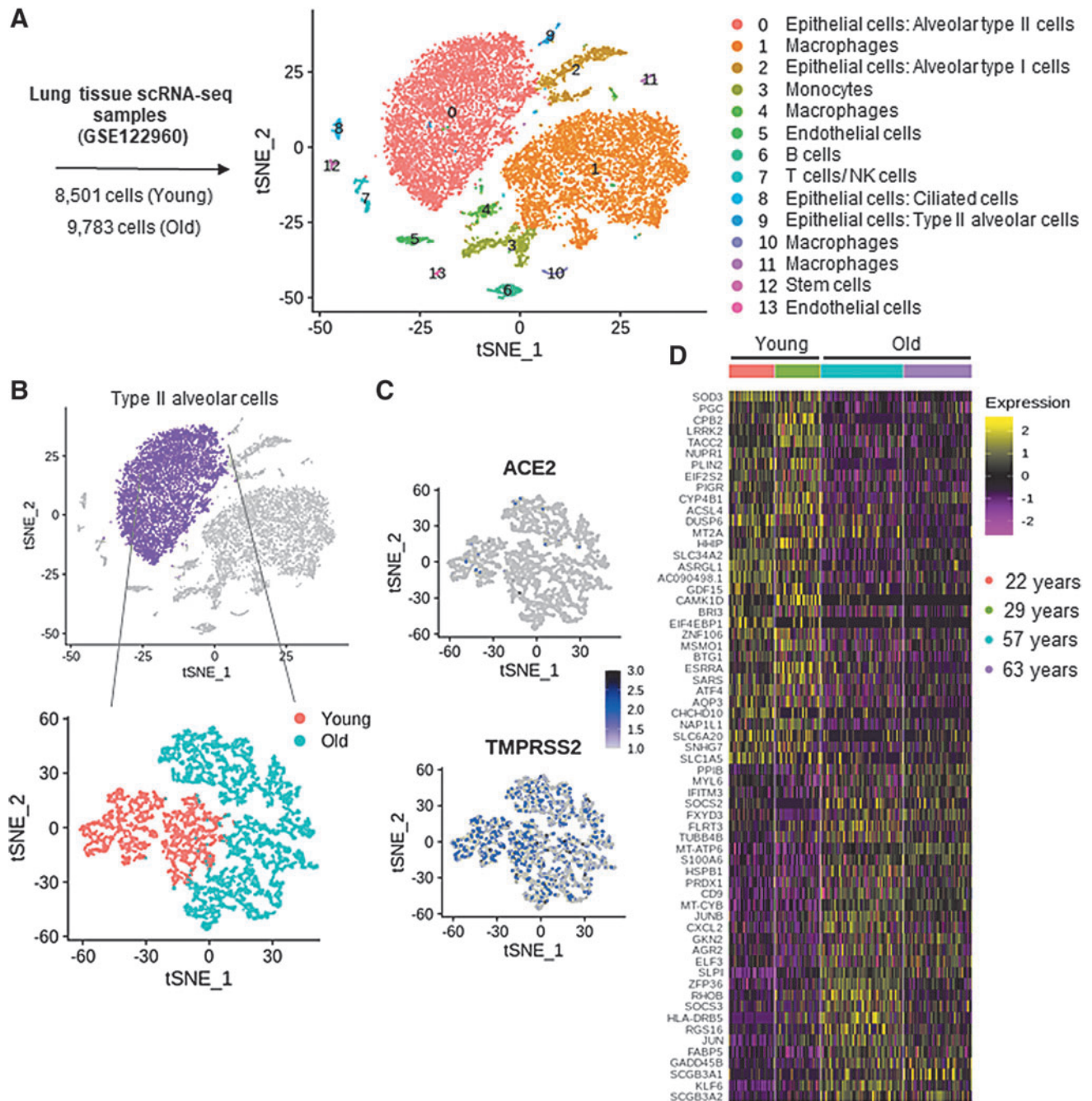


FIG. 1. Identification of 14 distinct clusters within the lung tissue with unique markers for each. (A) t-SNE projection of the filtered data (18,284 cells; 8501 young; 9783 old). Each cell is represented as a *dot*. (B) t-SNE clustering of the epithelial alveolar type II cells, cells showing clear separation between the cells from young and old groups. (C) Expression level of ACE2 (*top*) and TMPRSS2 (*bottom*) in alveolar type II cells. (D) Heatmap of the top differentially expressed genes between young and old lung alveolar type II cells (log fold change ± 0.4). Rows represent genes and columns represent cells. ACE2, angiotensin-converting enzyme 2; t-SNE, t-distributed stochastic neighbor embedding.

with marked inflammatory cell infiltration and alveolar hemorrhage (6). In the lungs, extracellular SOD3 is primarily expressed in bronchial and alveolar type II epithelial cells, alveolar macrophages, and pulmonary endothelial cells (4). Importantly, SOD3 mRNA expression in alveolar cells correlates with locally secreted enzyme activity, defending functional significance of observed changes in gene expression (27). With SOD3 as the top-ranked candidate, this study

identifies specific component of the alveolar cell antioxidant defense systems that are weakened in response to aging. Evidence in the current literature shows that SOD administration can decrease the severity of respiratory illness (7). Intravenous SOD administration in rabbit models reversed allergic emphysema (2). SOD-based therapies have also shown encouraging results in managing infectious diseases by improving host immune responses. Melon SOD restored

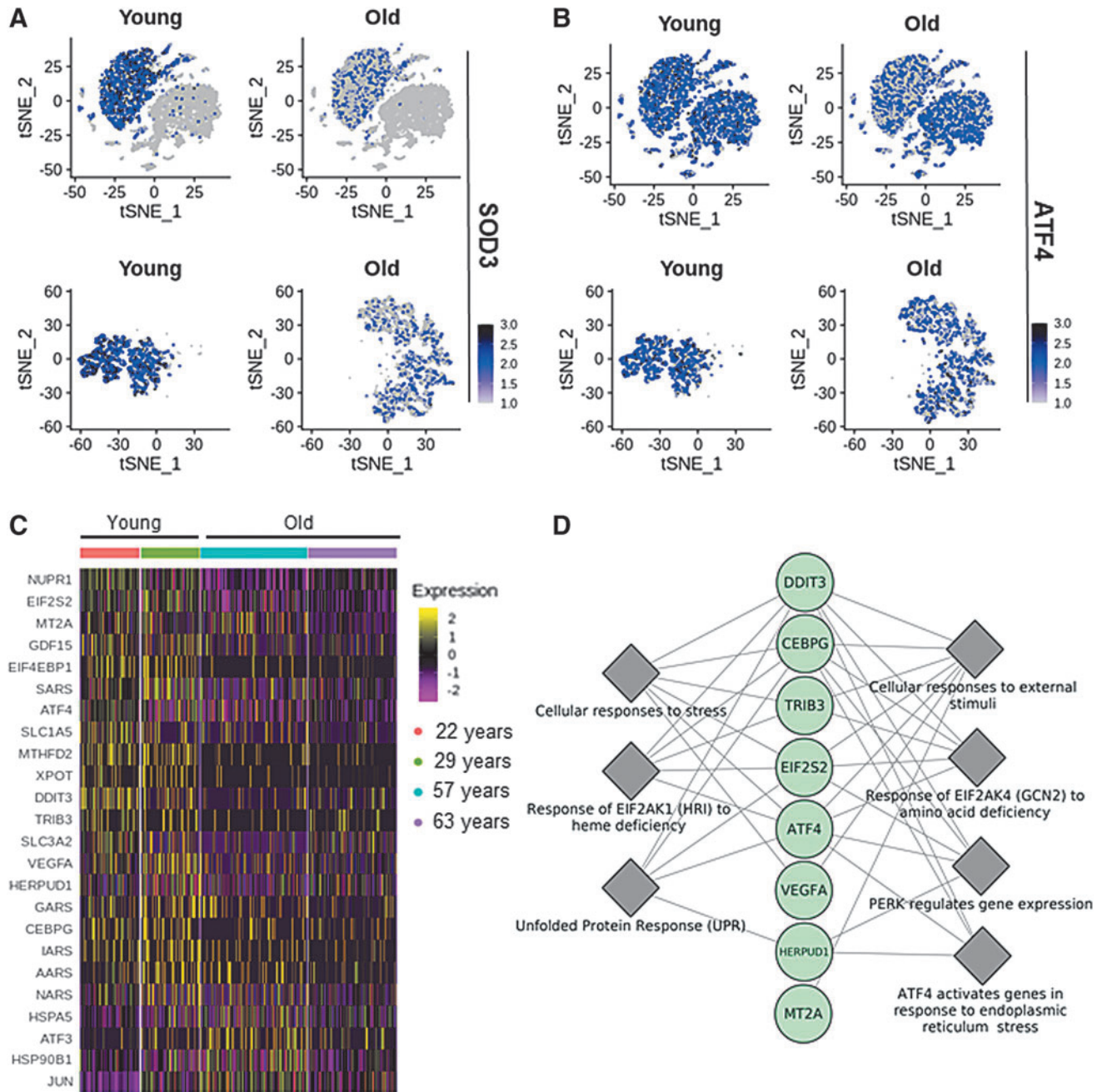


FIG. 2. Downregulation of *SOD3* and *ATF4* in alveolar type II cells of lungs from elderly donors. (A) t-SNE plots showing *SOD3* and (B) *ATF4* expression level between young and old age groups in (top) all the 14 clusters and (bottom) in alveolar type II cells. (C) Heatmap of the downstream targets of *ATF4*. Rows represent genes and columns represent cells. (D) Pathways enrichment for *ATF4* downstream targets that are downregulated in elderly. Circles represent genes and diamonds represent the enriched terms. *ATF4*, activating transcription factor 4; *SOD3*, superoxide dismutase 3.

CD4⁺/CD8⁺ ratio in cats infected with feline immunodeficiency virus (28). Cu/Zn-SOD significantly inhibited HIV replication (13). Cu/Zn-SOD inhalation protected murine lungs against pulmonary emphysema by decreasing ROS levels and proinflammatory cytokines expression (26). A limited-scale prospective double-blinded controlled trial NCT04323228 is about to start recruiting to test the effect of an antioxidant oral nutrition supplement in SARS-CoV 2 positive cases. All of these mentioned studies are preliminary at best and may help lay the foundation for a more serious

effort testing whether lung-specific delivery of *SOD3*-related antioxidants may work in synergy with promising antivirals such as remdesivir (NCT04323761) to further improve COVID-19 outcomes in the elderly.

Notes

Data acquisition

Primary single-cell RNA sequencing data were obtained from the GEO database (accession no. GSE122960). Authors

TABLE 1. REACTOME PATHWAYS ENRICHMENT FOR THE DOWNREGULATED GENES AMONG *ATF4* DOWNSTREAM TARGETS IN ALVEOLAR TYPE II CELLS FROM ELDERLY

<i>Pathway name</i>	<i>Reactions found/total reactions</i>	<i>FDR adjusted p-value</i>
Response of <i>EIF2AK1</i> (HRI) to heme deficiency	18/20	1.41E-14
<i>PERK</i> regulates gene expression	9/11	8.72E-12
Response of <i>EIF2AK4</i> (<i>GCN2</i>) to amino acid deficiency	13/16	4.01E-10
<i>ATF4</i> activates genes in response to endoplasmic reticulum stress	7/7	9.39E-09
Cellular responses to external stimuli	33/258	1.47E-08
Unfolded protein response	10/94	8.23E-08
Cellular responses to stress	27/227	1.03E-06

Pathways with adjusted *p*-value <2E-6 are shown.

EIF2AK1, eukaryotic translation initiation factor 2 alpha kinase 4; FDR, false discovery rate; *GCN2*, general control nonderepressible 2; *HRI*, heme-regulated inhibitor.

of the published study performed single-cell RNA sequencing on eight healthy donor lungs and nine lungs from patients with pulmonary fibrosis (20). Four samples were chosen from the healthy donor lungs in which two of them were 57 and 63 years old and the other two samples were from donors who were 22 and 29 years old. All four donors were females, nonsmokers, and African American.

Processing of raw data and quality control

All analyses were performed using Seurat package (v.3.1.1) in R (v.3.3.5) (22). The initial data set contained 20,163 cells from four lung samples (two young and two elderly). Gene expression values were log normalized using 10,000 transcripts per cell as scaling factor. Canonical correlational analysis was performed to integrate all four samples to identify the shared cell types using the top 2000 highly variable genes. Cells expressing <200 or >5000 genes, as detected, were excluded. Further filtering was performed to exclude cells that contain >15% of their reads from mitochondrial encoded genes. Cells with total number of counts between 2000 and 25,000 were kept for downstream analysis. After the filtration step, 18,284 cells (9783 from elderly and 8501 from young donors) were maintained for downstream analysis. Principal component analyses were performed and the first 15 principal components were chosen for clustering.

Determination of cell type identity

To identify cluster identity, SingleR package in R was used to calculate the similarity between each cluster and the HPCA data set (1). In addition, differential gene expression was performed between each cluster and the rest of the cells to identify cluster markers and further identification of the cluster identity using known markers from the literature.

Differential gene expression analysis

Differential gene expression analysis was performed for alveolar type II cells (cluster zero) to compare between young- and old-age groups using Wilcox-Rank Sum test with adjusted *p*-value <0.05. To avoid detection of genes only altered in one sample of either group, four additional comparisons were performed (each sample with the two samples from the other group). The genes that were not simultaneously upregulated or downregulated and in at least three such comparisons were excluded.

Ingenuity upstream regulator analysis in IPA

IPA (23,24,29) was used to identify the cascade of transcriptional regulators that can explain the observed gene expression changes in the data set. This approach is based on prior knowledge of expected effects between transcriptional regulators and their target genes. Two statistical measures (an overlap *p*-value and an activation *z*-score) were computed for each potential transcriptional regulator. The activation *z*-score was used to infer likely activation states of regulators based on comparison with a model that assigns random regulation directions.

Pathways enrichment

Reactome database (10) was used for enrichment of *ATF4* downstream targets that were found to be downregulated in alveolar type II cells in the cells from the elderly.

Authors' Contributions

A.S.A. and K.S. performed data analysis. A.S.A., K.S., H.M.E.A., and C.K.S wrote the article.

Funding Information

This work was supported in part by National Institutes of Health grants GM108014, NS042617 and NR015676.

Supplementary Material

- Supplementary Table S1
- Supplementary Figure S1
- Supplementary Figure S2

References

1. Aran D, Looney AP, Liu L, Wu E, Fong V, Hsu A, Chak S, Naikawadi RP, Wolters PJ, Abate AR, Butte AJ, and Bhattacharya M. Reference-based analysis of lung single-cell sequencing reveals a transitional profibrotic macrophage. *Nat Immunol* 20: 163–172, 2019.
2. Assa'ad AH, Ballard ET, Sebastian KD, Loven DP, Boivin GP, and Lierl MB. Effect of superoxide dismutase on a rabbit model of chronic allergic asthma. *Ann Allergy Asthma Immunol* 80: 215–224, 1998.
3. Castro SM, Guerrero-Plata A, Suarez-Real G, Adegboyega PA, Colasurdo GN, Khan AM, Garofalo RP, and Casola A.

- Antioxidant treatment ameliorates respiratory syncytial virus-induced disease and lung inflammation. *Am J Respir Crit Care Med* 174: 1361–1369, 2006.
4. Folz RJ, Guan J, Seldin MF, Oury TD, Enghild JJ, and Crapo JD. Mouse extracellular superoxide dismutase: primary structure, tissue-specific gene expression, chromosomal localization, and lung *in situ* hybridization. *Am J Respir Cell Mol Biol* 17: 393–403, 1997.
 5. Gharebaghi R, Heidary F, Moradi M, and Parvizi M. Metronidazole; a potential novel addition to the COVID-19 treatment regimen. *Arch Acad Emerg Med* 8: e40, 2020.
 6. Gongora MC, Lob HE, Landmesser U, Guzik TJ, Martin WD, Ozumi K, Wall SM, Wilson DS, Murthy N, Gravanis M, Fukai T, and Harrison DG. Loss of extracellular superoxide dismutase leads to acute lung damage in the presence of ambient air: a potential mechanism underlying adult respiratory distress syndrome. *Am J Pathol* 173: 915–926, 2008.
 7. Hernandez-Saavedra D, Swain K, Tuder R, Petersen SV, and Nozik-Grayck E. Redox regulation of the superoxide dismutases SOD3 and SOD2 in the pulmonary circulation. *Adv Exp Med Biol* 967: 57–70, 2017.
 8. Hoffmann M, Kleine-Weber H, Schroeder S, Kruger N, Herrler T, Erichsen S, Schiergens TS, Herrler G, Wu NH, Nitsche A, Muller MA, Drosten C, and Pohlmann S. SARS-CoV-2 cell entry depends on ACE2 and TMPRSS2 and is blocked by a clinically proven protease inhibitor. *Cell* 181: 271.e8–280.e8, 2020.
 9. Huang C, Wang Y, Li X, Ren L, Zhao J, Hu Y, Zhang L, Fan G, Xu J, Gu X, Cheng Z, Yu T, Xia J, Wei Y, Wu W, Xie X, Yin W, Li H, Liu M, Xiao Y, Gao H, Guo L, Xie J, Wang G, Jiang R, Gao Z, Jin Q, Wang J, and Cao B. Clinical features of patients infected with 2019 novel coronavirus in Wuhan, China. *Lancet* 395: 497–506, 2020.
 10. Jassal B, Matthews L, Viteri G, Gong C, Lorente P, Fabregat A, Sidiropoulos K, Cook J, Gillespie M, Haw R, Loney F, May B, Milacic M, Rothfels K, Sevilla C, Shamovsky V, Shorser S, Varusai T, Weiser J, Wu G, Stein L, Hermjakob H, and D'Eustachio P. The reactome pathway knowledgebase. *Nucleic Acids Res* 48: D498–D503, 2020.
 11. Khomich OA, Kochetkov SN, Bartosch B, and Ivanov AV. Redox biology of respiratory viral infections. *Viruses* 10, 2018.
 12. Kropski JA and Blackwell TS. Endoplasmic reticulum stress in the pathogenesis of fibrotic disease. *J Clin Invest* 128: 64–73, 2018.
 13. Lartigue A, Burlat B, Coutard B, Chaspoul F, Claverie JM, and Abergel C. The megavirus chilensis Cu,Zn-superoxide dismutase: the first viral structure of a typical cellular copper chaperone-independent hyperstable dimeric enzyme. *J Virol* 89: 824–832, 2015.
 14. Liu K, Chen Y, Lin R, and Han K. Clinical features of COVID-19 in elderly patients: a comparison with young and middle-aged patients. *J Infect* 2020 [Epub ahead of print]; DOI: 10.1016/j.jinf.2020.03.005.
 15. Liu Q, Zhou YH, and Yang ZQ. The cytokine storm of severe influenza and development of immunomodulatory therapy. *Cell Mol Immunol* 13: 3–10, 2016.
 16. Lukassen S, Chua RL, Trefzer T, Kahn NC, Schneider MA, Muley T, Winter H, Meister M, Veith C, Boots AW, Hennig BP, Kreuter M, Conrad C, and Eils R. SARS-CoV-2 receptor ACE2 and TMPRSS2 are primarily expressed in bronchial transient secretory cells. *EMBO J* e105114, 2020.
 17. Mehta P, McAuley DF, Brown M, Sanchez E, Tattersall RS, Manson JJ; and Hlth Across Speciality Collaboration UK. COVID-19: consider cytokine storm syndromes and immunosuppression. *Lancet* 395: 1033–1034, 2020.
 18. Olajuyin AM, Zhang X, and Ji HL. Alveolar type 2 progenitor cells for lung injury repair. *Cell Death Discov* 5: 63, 2019.
 19. Prevention CfDCA. 2020. Provisional death counts for coronavirus disease (COVID-19). <https://www.cdc.gov/nchs/nvss/vsrr/COVID19/2020>. Accessed April 17, 2020.
 20. Reyfman PA, Walter JM, Joshi N, Anekalla KR, McQuattie-Pimentel AC, Chiu S, Fernandez R, Akbarpour M, Chen CI, Ren Z, Verma R, Abdala-Valencia H, Nam K, Chi M, Han S, Gonzalez-Gonzalez FJ, Soberanes S, Watanabe S, Williams KJN, Flozak AS, Nicholson TT, Morgan VK, Winter DR, Hinchcliff M, Hrusch CL, Guzy RD, Bonham CA, Sperling AI, Bag R, Hamanaka RB, Mutlu GM, Yeldandi AV, Marshall SA, Shilatifard A, Amaral LAN, Perlman H, Sznajder JJ, Argento AC, Gillespie CT, Dematte J, Jain M, Singer BD, Ridge KM, Lam AP, Bharat A, Borade SM, Gottardi CJ, Budinger GRS, and Misharin AV. Single-cell transcriptomic analysis of human lung provides insights into the pathobiology of pulmonary fibrosis. *Am J Respir Crit Care Med* 199: 1517–1536, 2019.
 21. Richter K and Kietzmann T. Reactive oxygen species and fibrosis: further evidence of a significant liaison. *Cell Tissue Res* 365: 591–605, 2016.
 22. Satija R, Farrell JA, Gennert D, Schier AF, and Regev A. Spatial reconstruction of single-cell gene expression data. *Nat Biotechnol* 33: 495–502, 2015.
 23. Singh K, Pal D, Sinha M, Ghatak S, Gnyawali SC, Khanna S, Roy S, and Sen CK. Epigenetic modification of microRNA-200b contributes to diabetic vasculopathy. *Mol Ther* 25: 2689–2704, 2017.
 24. Singh K, Sinha M, Pal D, Tabasum S, Gnyawali SC, Khona D, Sarkar S, Mohanty SK, Soto-Gonzalez F, Khanna S, Roy S, and Sen CK. Cutaneous epithelial to mesenchymal transition activator ZEB1 regulates wound angiogenesis and closure in a glycemic status-dependent manner. *Diabetes* 68: 2175–2190, 2019.
 25. Tanaka K, Ishihara T, Azuma A, Kudoh S, Ebina M, Nukiwa T, Sugiyama Y, Tasaka Y, Namba T, Ishihara T, Sato K, Mizushima Y, and Mizushima T. Therapeutic effect of lecithinized superoxide dismutase on bleomycin-induced pulmonary fibrosis. *Am J Physiol Lung Cell Mol Physiol* 298: L348–L360, 2010.
 26. Tanaka K, Tanaka Y, Miyazaki Y, Namba T, Sato K, Aoshiba K, Azuma A, and Mizushima T. Therapeutic effect of lecithinized superoxide dismutase on pulmonary emphysema. *J Pharmacol Exp Ther* 338: 810–818, 2011.
 27. Vliet Avd. Antioxidant defenses in the lung. In: *Comparative Biology of the Normal Lung*, edited by Parent RA. San Diego, CA: Academic Press, 2015.
 28. Webb CB, Lehman TL, and McCord KW. Effects of an oral superoxide dismutase enzyme supplementation on indices of oxidative stress, proviral load, and CD4:CD8 ratios in asymptomatic FIV-infected cats. *J Feline Med Surg* 10: 423–430, 2008.
 29. Wisler JR, Singh K, McCarty AR, Abouhashem ASE, Christman JW, and Sen CK. Proteomic pathway analysis of

monocyte-derived exosomes during surgical sepsis identifies immunoregulatory functions. *Surg Infect (Larchmt)* 21: 101–111, 2020.

30. Zhang H, Zhou P, Wei Y, Yue H, Wang Y, Hu M, Zhang S, Cao T, Yang C, Li M, Guo G, Chen X, Chen Y, Lei M, Liu H, Zhao J, Peng P, Wang CY, and Du R. Histopathologic changes and SARS-CoV-2 immunostaining in the lung of a patient with COVID-19. *Ann Intern Med* 2020; DOI: 10.7326/M20-0533.

Address correspondence to:
Dr. Kanhaiya Singh
Indiana Center for Regenerative Medicine
and Engineering
Department of Surgery
Indiana University School of Medicine
Indianapolis, IN 46202
USA

E-mail: kanh@iu.edu

Date of first submission to ARS Central, April 19, 2020; date of acceptance, April 20, 2020.

Abbreviations Used

ACE2 = angiotensin-converting enzyme 2
 ATF4 = activating transcription factor 4
 ATOX1 = antioxidant 1 copper chaperone
 ATP7A = ATPase copper transporting alpha
 CAT = catalase
 COVID-19 = coronavirus disease 2019
 EIF2AK1 = eukaryotic translation initiation factor
 2 alpha kinase 4
 FDR = false discovery rate
 GCN2 = general control nonderepressible 2
 GPX1 = glutathione peroxidase 1
 HPCA = Human Primary Cell Atlas
 HRI = heme-regulated inhibitor
 M2TA = metallothionein 2A
 RNS = reactive nitrogen species
 ROS = reactive oxygen species
 SARS-CoV 2 = severe acute respiratory syndrome
 coronavirus 2
 scRNA-seq = single-cell RNA sequencing
 SOD = superoxide dismutase
 t-SNE = t-distributed stochastic neighbor embedding